

An effective approach to lane detection in driver assistance system

Gang-Yi JIANG, Suk-Kyo HONG, Tae-Young CHOI
Division of Electronics Engineering, Ajou University, KOREA
(Tel: +82-331-219-2330, Email: skhong@madang.ajou.ac.kr)

Abstract

An effective approach to lane detection in driver assistance system (DAS) is proposed, based on the decomposition of lane markings. The properties of the decomposed lane markings are discussed, and analyses on lane curvature are given. The current lane on road is detected quickly, the neighboring lane regions are also extracted for lane planning of the vehicle, and the parameters of lane structure are accurately estimated.

I. Introduction

The demand of traffic safety has been significantly increased with the growing number of vehicles on roads. Vision based DAS is helpful of solving traffic problems such as traffic safety, control of traffic flow, and so on. One of important functions in a DAS is to detect and track the lane boundaries or road. A number of lane detection techniques have been proposed. Broggi et al. have developed a parallel stereo vision system [1,2]. They detected road markings by morphological processing, overcame the annoying problems with non-uniform illumination, and implemented the detection step on massively parallel SIMD architectures. However, this system strongly relies on the implicit assumption of visible road markings, namely when no obstacles are on the path. Carnegie-Mellon University has developed the NAVLAB project for automatically driving [3]. Some DAS uses optical flow techniques to minimize the horizontal relative movement of lane markings with respect to the vehicle [4]. Techniques of recognizing road based on shape models have been proposed in Japan [5], and some AVL system with multi-resolution processing has been developed for autonomous steering control in Korea [6].

In this paper, lane markings of lane in the image plane are partitioned into upper-lane-markings and lower-lane-markings, according to the perspective effect. Their properties are discussed and exploited to extract lane markings. Then, an efficient algorithm to detect lane is

presented. Analyses of lane curvature are given and the lane structure parameters are accurately computed. Experimental results show that the new method performs lane detection well and reliably.

II. Effective Approach to Lane Detection

Fig.1(a) shows a typical road image of highway, where the road surface is divided into lanes by lane markings with dash shape and curve shape. The lane regions possess large areas, especially, the current lane has the largest area in all lanes in the image plane. The lane structures are quite long, and they are parallel in the real world. If a lane is straight without curvature in the real world, it will focus on a point, called vanishing point, along its top in the image plane. It is known that each pixel in the image plane represents different area in the real world due to the perspective effect. The pixels near the bottom of the image plane correspond to smaller areas in the real world, while those pixels close to the top correspond to larger areas and have more information about road. Fig.1(b) shows the extracted current lane in Fig.1(a), it is obvious that the lane markings close to the lower half of the image have more pixels, while the lane markings in the upper half of image possess smaller pixels. In fact, each segment of lane markings in real world is artificially designed to be of the same length and width. Moreover, highways and expressways are usually designed to have small curvature.

According to the above simple discussions, we partition lane markings into two parts: the part of $P_{L1}P_{L2}$ and $P_{R1}P_{R2}$ in Fig.1(c), called lower lane markings (LLMs), and the other part above the points P_{L2} and P_{R2} , referred to upper lane markings (ULMs). Consider the properties of LLMs and ULMs, we have

Property-1: LLMs are usually major parts of lane markings in the image plane, and they are longer and larger than ULMs due to the perspective effect.

Property-2: LLM represents the tangent of lane in the real world, while ULM describes the curvature of lane. In the image plane, the slope of left LLM is usually larger than

zero, whereas the slope of right LLM is less than zero.

Property-3: Two straight-line equations of LLMs intersect a point, which is an estimation of vanishing point and called as quasi-vanishing point (QVP). In the image plane, the distance between QVP and the joint of the left and right ULMs describes the degree of lane curvature. When lane goes straightly, the distance is near to zero. Conversely, if the distance is very large, it implies that the road curves largely. For road image sequences on highways, QVP varies without sudden changes if images are normally taken.

Property-4: The slopes of LLMs are mainly relative to the lateral offset. LLMs in the real world can be used to estimate the vehicle deviation angle.

Property-5: In the real world, LLMs are only minor parts of lane markings ahead of the vehicle, while ULMs are several times of LLMs.

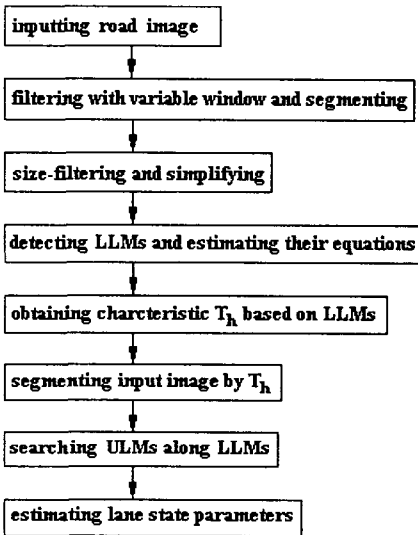


Fig.2 Diagram of lane detection

In our test system, only one CCD camera and radar modules are adopted as sensors in order to simplify the system. The CCD camera is used to capture road images in which lanes and obstacles are detected, and the radar module is used to help to locate obstacles ahead of the vehicle. A new algorithm is described in Fig.2. When a road image G_0 is inputted, it is filtered with variable window in Fig.3(b), which is obtained by simplifying the Mexican-hat window in Fig.3(a). The window width varies with the vertical coordinate of the filtered pixel, and defined by

$$\begin{cases} \tau = \tau_0 & v < v_0 \\ \tau = \tau_0 + k_0(v - v_0) & v_0 \leq v \leq v_1 \\ \tau = \tau_1 & v > v_1 \end{cases} \quad (1)$$

where τ_0, τ_1, v_0, v_1 and k_0 are constants, $\tau_0 > \tau_1, k_0 < 0$.

The filtered image G_f is segmented to obtain G_2 by T_1 , T_1 is defined by

$$T_1 = \bar{g}_1 + \frac{1}{N \times M} \sum_{(x,y)} |g_1(u,v) - \bar{g}_1| \quad (2)$$

where N and M are the dimensions of the image in pixel units, $0 \leq u < N$ and $0 \leq v < M$, and \bar{g}_1 denotes the expectation of $g_1(u,v)$ in G_f . Then, size-filtering and simplifying to the segmented image G_2 are performed, and the resultant image G_3 is used to extract LLMs' regions of the current lane. Furthermore, the straight-line equations of LLMs are estimated and QVP is also located. A characteristic T_h is calculated from the regions of LLMs in G_0 , it is exploited to segment G_0 in order to obtain an image G_4 . In G_4 , the ULMs of the current lane are searched along with the corresponding regions of LLMs. Finally, lane state analysis is performed and lane structure parameters are estimated accurately.

Moreover, neighboring ones of the current lane are also extracted in G_2 as additional information, which can be used for correcting the decision of lane direction and lane planning of the vehicle.

III. Analysis of Lane Curvature

From Fig.1(c), some simple analysis of lane curvature can be given due to the properties of LLMs and ULMs. If the joint point between two ULMs is very closed to the QVP, it implies that the ULMs and LLMs have the identical direction, the lane goes straightforwardly without curvature. If the joint point between two ULMs is far from the QVP, and if the left ULM is below the extended line of the left LLM and the right ULM is above the extended line of the right LLM, then the lane may turn right. Conversely, the lane may turn left.

The other way to analyze of lane curvature is based on pattern matching. Fig.4 shows that lanes are divided into three groups of lane patterns: without initial lateral offset, with positive initial lateral offset and with negative initial lateral offset. Each group consists of three situations: straight lane, lane with left curve, and lane with right curve, each pattern has different lane state parameters. Then, when an unknown lane pattern is inputted, it can be recognized by pattern matching with the known patterns.

To obtain precise estimation of the lane curvature, a geometric model in Fig.5 is adopted. In the figure, x_0, z_0, γ and θ denote lateral offset of vehicle, camera height from ground, vehicle deviation angle, and inclination camera angle, respectively. With inverse-perspective

transform, a point $P(u,v)$ in the image plan is mapped into $Q(x,y,z)$ in the real world, and expressed by

$$x = \frac{uz_0}{v \cos \theta - f \sin \theta}, \quad (3a)$$

$$y = \frac{z_0(f \cos \theta + v \sin \theta)}{v \cos \theta - f \sin \theta}, \quad (3b)$$

$$z = z_0. \quad (3c)$$

Then, the lateral offset and curvature of lane are computed in the real world rather than the image plane. Fig.6 shows a lane with curvature in the real world, where $z=z_0$. It is clear that the later offset $x_0(y)$ varies with the vertical distance from the vehicle. The line AC is the extension of the right LLM. Let $AB=\Delta y$, $BD=\Delta x$, and $BE=\Delta x_1$, then the vehicle deviation angle, $\gamma=\angle BAC$, and the radius R of the curve AD are represented by

$$\gamma = a \tan\left(\frac{\Delta x_1}{\Delta y}\right) \quad (4)$$

$$R = \frac{r^2 + (\Delta x - \Delta x_1)^2 - 2r(\Delta x - \Delta x_1) \sin \gamma}{2r(\Delta x - \Delta x_1) \cos \gamma} \quad (5)$$

where $r^2=(\Delta y)^2+(\Delta x_1)^2$.

IV. Experimental Results

In order to evaluate the effectiveness of this approach, a numerous experiments have been implemented with our experimental system. The test images taken by a CCD camera are 320×240 in size with 256 gray levels. For the input image in Fig.1(a), some resultant images are shown in Fig.7. Fig.7(a) and (b) give the filtered image G_1 , obtained by using variable window in Fig.3(b), and its segmented image G_2 . After size-filtering and simplifying G_2 , the processed image G_3 is obtained in Fig.7(c). Then the LLMs are extracted, and their straight-line equations are estimated and marked with gray line in Fig.7(c). The characteristic parameter T_h is obtained from the LLMs' regions in the input image G_0 , and it is exploited to segment G_0 to obtain a binary image G_4 in Fig.7(d). ULMs are searched along LLMs in G_4 . Fig.1(b) shows the extracted lane markings of the current lane. Fig.7(e) shows the result, obtained by the inverse-perspective transform, in which the gray line and white lane express the straight-line equations of LLMs and the lane markings, respectively. The straight-line equations of LLMs indicate that the lane tangent bends to the right, and the estimated vehicle deviation angle γ is 0.79° . The radius of the lane curvature is about 520.12m, and the lane width is about 3.78m. The lateral offsets at 10m, 20m, 30m, and 40m in front of the vehicle are 0.15m, 0.39m, 0.85m, and 1.52m,

respectively. In addition, the neighboring lanes of the current lane can be extracted by region detection from Fig.7(b) and (d), and shown in Fig.7(f). The information of the neighboring lanes will be helpful of determining lane planning of the vehicle. From Fig.7, the left ULM is below the extension of the left LLM while the right ULM is above the extension of the right LLM, it means that the current lane curves right. Moreover, it is clear that the current lane pattern corresponds to the third pattern of the first row in Fig.4. These analyses of lane curvature agree with the above computation of the lane curvature.

Fig.8 shows other results, Fig.8(a) is a road image in which the current lane sides have been found and marked with red color. Fig.8(b) is the segmented image by T_h , in which DLMs and ULMs have been located. Fig.8(c) gives the labeled lane regions, it also shows that some obstacles may exist in the neighboring lanes. Combining the input image, the obstacles can be detected. The road is straightforward without curvature. The width of the current lane is 3.72m, γ is -0.40° , and the lateral offsets at 10m, 20m, 30m, and 40m in front of the vehicle are 0.30m, 0.27m, 0.21m, and 0.15m, respectively.

V. Conclusions

In terms of the perspective effect, we have decomposed the lane markings of the current lane in the image plane into LLMs and ULMs, and discussed their properties. Then, a new algorithm to detect lanes is proposed, based on LLMs and ULMs. Analyses of lane curvature are given, and the parameters of lane structure are accurately estimated. To get additional information for deciding lane planning of the vehicle, the neighboring lanes of the current lane are also extracted. Experimental results show that the new approaches can perform lane detection well and reliably.

References

- [1] M. Bertozzi, A. Broggi, and A. Fascioli, "Autonomous Vehicles", Linux Journal, 59:40-45, 1999
- [2] D. Pomerleau, "RALPH: Rapidly Adapting Lateral Position Handler", Proc. of IEEE Symposium on Intelligent Vehicles, Sept. Detroit, 506-511, 1995
- [3] D. Raviv, M. Herman, "A new approach to vision and control for road following", Proc. of CVPR, 217-225, 1991,
- [4] K. Uchimura, Z. C. Hu, "Recognition of Shape Models for General Roads", Proc. of ACCV, 519-526, 1998
- [5] C. W. Shin, K. I. Kin, "Design of real-time image processing board with multi-resolution processing method for ALV", Proc. of ITSC, CD-version, Seoul, 1998

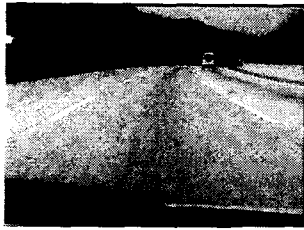
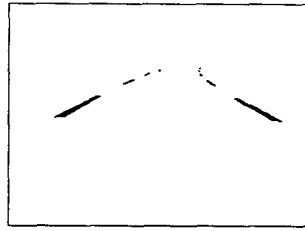
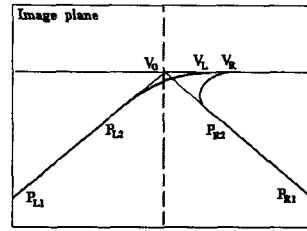


Fig.1 (a) A road image,



(b) The current lane,



(c) Lane model in image plane.

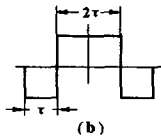
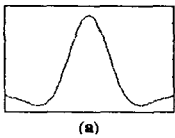


Fig.3 Filtering window.

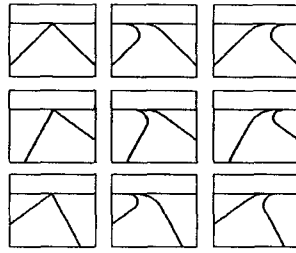


Fig.4 Patterns of lane curvature.

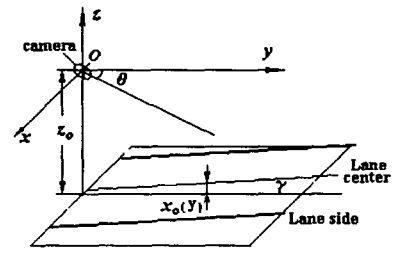


Fig.5 Geometric model

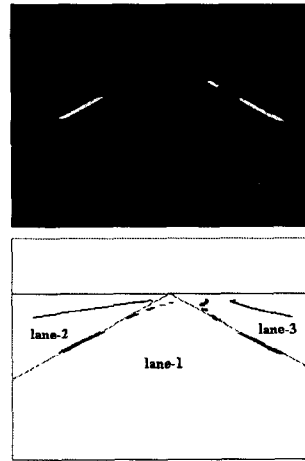
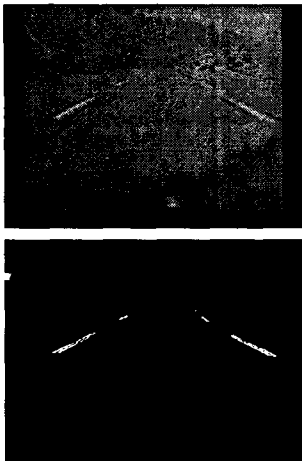


Fig.7 (a) Filtered image G_1 , (b) Segmented image G_2 ,
(c) Size-filtered image G_3 , (d) Processed image G_4 by T_h ,
(e) Inverse-perspective transformed image, (f) Labeled lane regions.

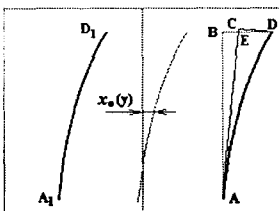


Fig.6 Lane model
in the real world.

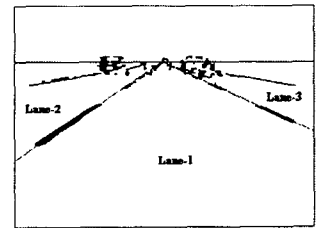


Fig.8 Other results, (a) a road image, the current lane sides are marked with red color,
(b) The segmented image, where DLMS and ULMS have been located,
(c) Labeled lane regions, where obstacles may exist in the neighboring lanes.